COMPARISON OF WELL-POSEDNESS CRITERIA OF TWO-FLUID MODELS FOR NUMERICAL SIMULATION OF GAS-LIQUID TWO-PHASE FLOWS IN VERTICAL PIPES

by

Falahati NAGHIBI, Vahid SHOKRI*, and Alireza MAJIDIAN

Department of Mechanical Engineering, Sari Branch, Islamic Azad University, Sari, Iran

Original scientific paper
https://doi.org/10.2298/TSCI200420158F

The purpose of the present study is to compare the well-posedness criteria of the free-pressure two-fluid model, single-pressure two-fluid model, and two-pressure two-fluid model in a vertical pipe. Two-fluid models were solved using the conservative shock capturing method. A water faucet case is used to compare two-fluid models. The free pressure two-fluid model can accurately predict discontinuities in the solution field if the problem's initial condition satisfies the Kelvin Helmholtz instability conditions. The single-pressure two-fluid model can accurately predict the behavior of flows in which the two phases are poorly coupled. The two-pressure two-fluid model is an unconditionally well-posed one. If in the free-pressure two-fluid model and single-pressure two-fluid model, the range of velocity difference of two phases exceeds certain limits, the models will be ill-posed. The two-pressure two-fluid model produces more numerical diffusion than the free-pressure two-fluid and single-pressure two-fluid models in the solution field. High numerical diffusion of two-pressure two-fluid models leads to failure to better comply with the problem's analytical solution. Results show that a single-pressure model is a powerful model for numerical modeling of gas-liquid two-fluid-flows in the vertical pipe due to a broader range of well-posed than free-pressure models and less numerical diffusion than the two-pressure mode.

Key words: *two-fluid model, two-phase flow, well-posedness, numerical modeling*

Introduction

The investigation of two-phase fluid-flow is an essential aspect of applied researches and industrial applications. In nuclear power plants, the two-phase water-flow is a crucial component of the system because the water in its liquid-gas two-phase form is used as a coolant and a moderator in reactor cores. Also, this flow type appears in other equipment of nuclear reactors, including turbine, condenser, and heat exchanger. Hence, obtaining the most favorable design for such applications requires a concrete understanding of two-phase fluid--flow physics's underlying characteristics and mathematical modeling.

In numerical modeling of two-phase flows, selecting an appropriate mathematical model is one of the significant challenges. Identifying and evaluating the selected model's restrictions is essential for a more accurate prediction of two-phase flows.

* Corresponding author, e-mail: shokri.vhd@iausari.ac.ir

Using 3-D Navier-Stokes equations is very costly for analyzing two-phase flows. As a result, various models are being used to simplify these equations. Despite the heavy literature on mathematical models for such flows, the most widely used models fall into three following categories [1]: homogeneous equilibrium model, drift-flux model, and two-fluid model.

Among these models, the most comprehensive model is the two-fluid model [2]. The model that we will focus on in this work is the two-fluid model.

Although the two-fluid model has successfully been used in simulating two-phase flow in a pipeline, the two-fluid model suffers from an ill-posedness issue. When the relative velocity between gas and liquid phases surpasses a critical value, the governing equations lose their realistic characteristics [3]. Complex roots suggest an elliptic equation system that results in the two-fluid model's ill-posedness because only the initial conditions can be specified in the temporal direction. Any infinitesimal disruption will cause exponential growth of the waves without any limit [3]. This ill-posedness situation suggests that the two-fluid model cannot correctly predict the pipe's realistic flow features. Therefore, for this model's meaningful results, the magnitude of relative velocity between gas and liquid phases must be smaller than a critical value, which depends on the liquid level, gravity, and other flow properties [3].

So far, many solutions have been suggested to eliminate or reduce the two-fluid model's ill-posedness problem. One of these solutions is to present different assumptions for the pressure of phases and pressure correction term. There are various types of two-fluid models, and being ill-posed or well-posed of their governing equations is the criteria for their categorizing. Types of the two-fluid models are presented: free-pressure model [4], single-pressure model [5], and two-pressure model [6].

Since most two-fluid models are non-conservative, it is recommended to use a particular two-fluid model. Watson [4] proposed a model that significantly reduced the numerical complexity. This model assumed the gas and liquid phases are incompressible and the fluids treated as a two-phase mixture that flows through a gravitationally separated configuration. In this area, some researchers used the free pressure two-fluid model [7-11].

Woodburn and Issa [12] has proposed a new methodology and Issa and Kempf [13] called the *slug capturing* technique in which the slug flow regime is predicted by solving the conservation equation. This technique utilizes an Eulerian approach for solving the 1-D two-fluid model and can capture the development of hydrodynamic instabilities and the growth and collapse of the slugs.

In Woodburn and Issa [12] two-fluid model, it is assumed that phase pressure and phase pressure at the interface are equal [13]. The gas phase and liquid phase pressures are shown as P_g and P_l, respectively. Moreover, they assumed $P = P_g = P_l$, and gas and liquid pressures are equal at the interface ($P = P_{gi} = P_{li}$). The P_{gi} and P_{li} are gas and liquid phase pressures at the interface, respectively. It means that the pressure of gas phase and the pressure of liquid phase are assumed to be the same and the whole two-phase system is modeled with a single pressure:

$$P = P_g = P_{gi} = P_l = P_{li} \tag{1}$$

Issa and Kempf [13] assumed that the gas phase and liquid phase pressures at the interface are the same (*i.e.*, $P_{gi} = P_{li}$) [12]. Furthermore, they considered that the liquid phase pressure in the vertical direction varies hydrostatically. They used the hydrostatic pressure correction term in their study [12].

$$P = P_{\mathrm{g}} = P_{\mathrm{gi}} = P_{\mathrm{li}} \tag{2}$$

$$P_{\mathrm{l}}(y) = P + \rho_{\mathrm{l}}\,\mathrm{G}\,(h_{\mathrm{l}} - y)\cos\beta \tag{3}$$

where P is the gas phase pressure and $P_{\mathrm{l}}(y)$ – the liquid phase pressure. Also, ρ_{l}, G, h_{l}, and β are liquid phase density, gravitational acceleration constant, level of the liquid phase, and the pipe's inclination, respectively.

Other researchers used the single-pressure two-fluid model for numerical modeling of two-phase flows by applying the hydrostatic pressure correction term [12, 14-21].

Evje and Flatten [22] implemented the Roe scheme to a four-equation single-pressure two-fluid model and showed that the second-order extension based on wave decomposition and flux-difference splitting gives improved results in comparison of the first-order scheme. They considered the gas phase is compressible and the liquid phase is incompressible. As well, they considered the following assumptions for pressure:

$$P = P_{\mathrm{g}} = P_{\mathrm{l}} \tag{4}$$

$$P_{\mathrm{i}} = P_{\mathrm{gi}} = P_{\mathrm{li}} \tag{5}$$

where P is the phase pressure (in this model, the pressure of two phases are assumed equal) and P_{i} – the pressure at the interface. In their two-fluid model, the relationship between phase pressure and pressure at the interface of phases was stated by the hydrodynamic pressure correction term presented by Paillere *et al.* [23]. Other researchers used the single-pressure two-fluid model with hydrodynamic pressure correct terms [20, 21, 24-26].

A two-pressure two-fluid model has a particular structure, and its analysis is more complicated than the analysis of a basic single-pressure two-fluid model. Moreover, a two-pressure two-fluid model is always a hyperbolic one [6]. There are two two-pressure two-fluid models for isotherm flows [27].

The first model is described through four differential equations in which pressures in both phases are considered equal, while the second model is expressed through five differential equations in which the pressures in two phases are different [27]. Usually, two-fluid models containing four equations have complex eigenvalues. As a result, these equations are not well-posed. Thus, to solve these models numerically, the high artificial viscosity must be inserted into the models [6].

Ransom and Hicks [6] presented a compressible two-fluid model having five differential equations. They stated that for having a two-fluid model that is always hyperbolic, the assumption of pressure equality in two phases must change. In their model, Ransom and Hicks [6] did not use the pressure relaxation method. In their model, the pressure of phases varies over time. Saurel and Abgrall [28] proposed a two-pressure two-velocity two-phase model. In this model, which has seven equations, the pressure and velocity relaxations can be carried out following the hyperbolic time step. This model can be considered an expansion of Baer and Nunziato's [29] model.

Fontalvo *et al.* [30] assess closure relations' effect in a 1-D two-fluid model on annular vertical flows. They discretized conservation equations by first-order, first-order upwind, and second-order schemes. They performed a mesh sensitivity analysis to show the advantages and disadvantages of the aforementioned schemes and investigated the effect of closure relations on well-posedness and physical representativeness. Best closures predictions showed an average error of 9% and 22% for pressure gradient and liquid holdup. They also

showed that, despite the vertical annular flow complexity, the model could predict wave formation and propagation quite well [30].

Saraswat *et al.* [31] analyzed the linear stability of the RELAP5 two-fluid model used to simulate transient two-phase flow to investigate the ill-posedness of the RELAP5 model for normal and accident situations in a water reactor. They introduced a new term called bubble collision to the two-fluid model to improve its results. It is showed that the addition of the bubble collision to RELAP5 makes the model unconditionally well-posed [31].

In numerical solution of two-phase flows, due to a deformable interface, the fluid properties vary discontinuously during passing through the interface. The selection of a proper that can predict the discontinuities during passing through the interface is critical. According to reviewing the literature, it is clear that, in numerical modeling of isothermal two-phase gas--liquid flows, free pressure two-fluid models, single-pressure or two pressure have been used. Each of the two-fluid models has different criteria of well-posedness that directly influence the accuracy of the solution. However, comparing two-fluid models and the well-posedness criteria of two-fluid models and their effects on the numerical solution results have never been demonstrated. This is realized in the present work.

Governing equations

The main focus of this work is the two-fluid model. In this model, each phase is characterized by continuity and momentum equations, while the gas and liquid phases' interaction is expressed via particular closure relations. This model treats each phase as a distinct fluid with its governing equations.

Moreover, dynamic interaction between phases is calculated by inter-phase forces that are appeared in the conservation equations by the source term. In this study, the flow is considered isothermal.

According to the assumptions for the pressure term, the conservation and momentum equations are presented for different forms of the two-fluid model as following:

Single-pressure model

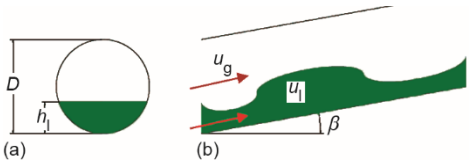

Figure 1. Side view of the two-phase flow pipe; (a) initial condition and (b) one instant during the transient

The single-pressure model is a non-conservative form of the two-fluid model presented by Evje and Flatten [22]. The single-pressure model consists of four differential equations, including two mass equations and two momentum equations for each phase. In the single-pressure model, gas and liquid phases are considered as compressible and incompressible, respectively. Equations of the single-pressure model are presented as follows. A typical side view of a two-phase flow pipe is shown in fig. 1.

Mass equation of gas:

$$\frac{\partial}{\partial t}(\rho_g R_g) + \frac{\partial}{\partial x}(\rho_g R_g u_g) = 0 \tag{6a}$$

Mass equation of liquid:

$$\frac{\partial}{\partial t}(\rho_{\mathrm{l}} R_{\mathrm{l}}) + \frac{\partial}{\partial x}(\rho_{\mathrm{l}} R_{\mathrm{l}} u_{\mathrm{l}}) = 0 \tag{6b}$$

Momentum equation of gas:

$$\frac{\partial}{\partial t}(\rho_{\mathrm{g}} R_{\mathrm{g}} u_{\mathrm{g}}) + \frac{\partial}{\partial x}(\rho_{\mathrm{g}} R_{\mathrm{g}} u_{\mathrm{g}}^2) = -\frac{\partial}{\partial x}[(P_{\mathrm{g}} - P_{\mathrm{gi}}) R_{\mathrm{g}}] - R_{\mathrm{g}} \frac{\partial P_{\mathrm{gi}}}{\partial x} - \rho_{\mathrm{g}} R_{\mathrm{g}} \mathrm{G}\sin\beta + F_{\mathrm{gw}} + F_{\mathrm{i}} \tag{6c}$$

Momentum equation of liquid:

$$\frac{\partial}{\partial t}(\rho_{\mathrm{l}} R_{\mathrm{l}} u_{\mathrm{l}}) + \frac{\partial}{\partial x}(\rho_{\mathrm{l}} R_{\mathrm{l}} u_{\mathrm{l}}^2) = -\frac{\partial}{\partial x}[(P_{\mathrm{l}} - P_{\mathrm{li}}) R_{\mathrm{l}}] - R_{\mathrm{l}} \frac{\partial P_{\mathrm{li}}}{\partial x} - \rho_{\mathrm{l}} R_{\mathrm{l}} \mathrm{G}\sin\beta + F_{\mathrm{lw}} - F_{\mathrm{i}} \tag{6d}$$

where for k^{th} phase ($k = g$ is for gas phase and $k = l$ is for liquid phase), ρ_k – the density of the k^{th} phase, and R_k – the volume fraction of the k^{th} phase, u_k – is the velocity of k^{th} phase, P_k – the pressure of k^{th} phase, P_{ki} – the pressure of the k^{th} phase at the interface, β – the pipe's inclination, and G – the gravitational acceleration. The friction force of each phase at the walls F_{kw} (w refers to the wall) and F_i is the friction force between phases at their interface. In fig. 1, D and h_l are the pipe diameter and the height of the liquid phase, respectively.

In our model, the gas and liquid phases pressures are the same (*i.e.*, $P_g = P_l = P$) and the pressure of phases at the interface are equal (*i.e.*, $P_{gi} = P_{li} = P_i$) Therefore, eqs. (6c) and (6d) are rewritten:

$$\frac{\partial}{\partial t}(\rho_{\mathrm{g}} R_{\mathrm{g}} u_{\mathrm{g}}) + \frac{\partial}{\partial x}(\rho_{\mathrm{g}} R_{\mathrm{g}} u_{\mathrm{g}}^2 + R_{\mathrm{g}} P) = P_{\mathrm{i}} \frac{\partial R_{\mathrm{g}}}{\partial x} - \rho_{\mathrm{g}} R_{\mathrm{g}} \mathrm{G}\sin\beta + F_{\mathrm{gw}} + F_{\mathrm{i}} \tag{6e}$$

$$\frac{\partial}{\partial t}(\rho_{\mathrm{l}} R_{\mathrm{l}} u_{\mathrm{l}}) + \frac{\partial}{\partial x}(\rho_{\mathrm{l}} R_{\mathrm{l}} u_{\mathrm{l}}^2 + R_{\mathrm{l}} P) = P_{\mathrm{i}} \frac{\partial R_{\mathrm{l}}}{\partial x} - \rho_{\mathrm{l}} R_{\mathrm{l}} \mathrm{G}\sin\beta + F_{\mathrm{lw}} - F_{\mathrm{i}} \tag{6f}$$

In momentum equations, the term $P - P_i$ is indicated as ΔP and called the pressure correction term, and the following relation is presented for its calculation [23, 32]:

$$\Delta P = P - P_i = \delta \frac{R_{\mathrm{l}} R_{\mathrm{g}} \rho_{\mathrm{l}} \rho_{\mathrm{g}}}{\rho_{\mathrm{g}} R_{\mathrm{l}} + \rho_{\mathrm{l}} R_{\mathrm{g}}} (u_{\mathrm{g}} - u_{\mathrm{l}})^2 \tag{7}$$

where $\delta = 1.2$ [22]. Unknowns in the single-pressure equation system are ρ_g, R_g, R_l, u_g, u_l, P and for closing equation system, additional equations are required.

Two more relationships are required to complete the mass and momentum eqs. (6a)-(6d). The first relationship is derived from the geometric constraint where the whole pipe is filled by the gas and liquid phases [22], hence:

$$R_{\mathrm{l}} + R_{\mathrm{g}} = 1 \tag{8}$$

Moreover, appropriate thermodynamic sub-models must be specified. For phase k, the simplified linear thermodynamic relations can be assumed [22].

$$\rho_k = \rho_{0,k} + \frac{P_k - P_{0,k}}{C_k^2} \tag{9}$$

where $\rho_{0,k}$ and $P_{0,k}$ are the given values for density and pressure, respectively. The C_k is the speed of sound in each phase and is considered [22]:

$$\frac{\partial P_k}{\partial \rho_k} = C_k^2 \tag{10}$$

The assumption that C_k is constant, states that the flow is isentropic. Throughout this work, we use the following parameters for the liquid phase [22]:

$$P_{0,\mathrm{l}} = 10^5\,\mathrm{Pa} \quad \rho_{0,\mathrm{l}} = 1000\ \mathrm{kg/m^3} \text{ and } C_{\mathrm{l}}^2 = 10^6\,\mathrm{m/s^2}$$

For the gas phase, we specify:

$$P_{0,\mathrm{g}} = 0 \quad \rho_{0,\mathrm{g}} = 0 \text{ and } C_{\mathrm{g}}^2 = 10^5\,\mathrm{m/s^2}$$

Two-pressure two-fluid model

The two-pressure model is a non-conservative type of two-fluid model introduced by Ransom and Hicks [6]. Then, this model was improved by Saurel and Abgrall [28]. The two--fluid model consists of five differential equations, including two equations for the continuity and two equations for the momentum, and one equation for the volume fraction's Advection. In the two-pressure model, both gas and liquid phases are considered as compressible. Equations of the isothermal two-pressure are presented as following.

– Advection of volume fraction

$$\frac{\partial R_{\mathrm{g}}}{\partial t} + u_{\mathrm{i}} \frac{\partial R_{\mathrm{g}}}{\partial x} = r_{\mathrm{P}}(P_{\mathrm{g}} - P_{\mathrm{l}}) \tag{11a}$$

– Mass equation of gas

$$\frac{\partial}{\partial t}(\rho_{\mathrm{g}} R_{\mathrm{g}}) + \frac{\partial}{\partial x}(\rho_{\mathrm{g}} R_{\mathrm{g}} u_{\mathrm{g}}) = 0 \tag{11b}$$

– Mass equation of liquid

$$\frac{\partial}{\partial t}(\rho_{\mathrm{l}} R_{\mathrm{l}}) + \frac{\partial}{\partial x}(\rho_{\mathrm{l}} R_{\mathrm{l}} u_{\mathrm{l}}) = 0 \tag{11c}$$

– Momentum equation of gas

$$\begin{aligned}\frac{\partial}{\partial t}(\rho_{\mathrm{g}} R_{\mathrm{g}} u_{\mathrm{g}}) + \frac{\partial}{\partial x}(\rho_{\mathrm{g}} R_{\mathrm{g}} u_{\mathrm{g}}^2) = -R_{\mathrm{g}} \frac{\partial P_{\mathrm{g}}}{\partial x} - \frac{\partial}{\partial x}[(P_{\mathrm{g}} - P_{\mathrm{gi}}) R_{\mathrm{g}}] - \\ -R_{\mathrm{g}} \rho_{\mathrm{g}}\, \mathrm{G} \sin\beta + r_{\mathrm{v}}(u_{\mathrm{g}} - u_{\mathrm{l}}) + F_{\mathrm{gw}} + F_{\mathrm{i}}\end{aligned} \tag{11d}$$

– Momentum equation of liquid

$$\begin{aligned}\frac{\partial}{\partial t}(\rho_{\mathrm{l}} R_{\mathrm{l}} u_{\mathrm{l}}) + \frac{\partial}{\partial x}(\rho_{\mathrm{l}} R_{\mathrm{l}} u_{\mathrm{l}}^2) = -R_{\mathrm{l}} \frac{\partial P_{\mathrm{l}}}{\partial x} - \frac{\partial}{\partial x}[(P_{\mathrm{l}} - P_{\mathrm{li}}) R_{\mathrm{l}}] - \\ -R_{\mathrm{l}} \rho_{\mathrm{l}}\, \mathrm{G} \sin\beta + r_{\mathrm{v}}(u_{\mathrm{g}} - u_{\mathrm{l}}) + F_{\mathrm{lw}} - F_{\mathrm{i}}\end{aligned} \tag{11e}$$

In the two-pressure model, the liquid phase and gas phase pressures at the interface are considered as equal (*i.e.* $P_{gi} = P_{li} = P_i$). Therefore, eqs. (11d) and (11e) are rewritten:

$$\frac{\partial}{\partial t}(\rho_g R_g u_g) + \frac{\partial}{\partial x}(\rho_g R_g u_g^2 + R_g P_g) = P_i \frac{\partial R_g}{\partial x} - R_g \rho_g G \sin\beta + r_v(u_g - u_l) + F_{gw} + F_i \quad (11f)$$

$$\frac{\partial}{\partial t}(\rho_l R_l u_l) + \frac{\partial}{\partial x}(\rho_l R_l u_l^2 + R_l P_l) = P_i \frac{\partial R_l}{\partial x} - R_l \rho_l G \sin\beta + r_v(u_g - u_l) + F_{lw} - F_i \quad (11g)$$

In momentum equations, the term $P - P_i$ is called the pressure correction term, and the following relations are presented to calculate this term [28]:

$$P - P_i = \delta \frac{R_l R_g \rho_l \rho_g}{\rho_g R_l + \rho_l R_g}(u_g - u_l)^2 \quad (12)$$

The unknown in two-pressure equations are ρ_g, ρ_l, R_g, R_l, u_g, u_l, P_g, and P_l. Furthermore, for closing the equation system, other relations are required. The first relation is a geometric constraint that uses eq. (8). In addition to eq. (8), for closing the system, thermodynamic sub-models are required that use eqs. (9) and (10).

In where u_i is the average interface velocity that is calculated as following [28]:

$$u_i = \frac{\sum_{\forall k} \rho_k R_k u_k}{\sum_{\forall k} \rho_k u_k} \quad (13)$$

where r_v is a velocity-relaxation parameter. If the value of r_v is too high, phasic velocities of two phases become equal. In present work, we do not consider the velocity relaxation, and subsequently:

$$r_v \equiv 0 \quad (14)$$

where r_P is a pressure-relaxation parameter. For $r_P = 0$, the phasic pressures of two phases are linearly independent and as $r_P \to \infty$, they become equal.

For many two-phase flows, especially in a slug flow, the phases' pressure is not independent [27]. This dependence is addressed by the pressure-relaxation procedure [27]. Two pressure relaxation procedures are discussed as following [28].

Finite pressure-relaxation procedure

The source term in eq. (11a) is significant, and we need to solve a five-equations system utilizing an appropriate numerical procedure [27]. Here, we utilize a fractional-step technique: Primarily, the *hyperbolic part* of the equations system (11a)-(11e) (that is, with $r_P = 0$) is advanced one step, Δt. Next, the *relaxation part* is considered:

$$\frac{\partial R_g}{\partial t} = r_P(P_g - P_l) \quad (15)$$

$$\frac{\partial}{\partial t}(\rho_k R_k) = 0 \quad (16)$$

$$\frac{\partial}{\partial t}(\rho_k R_k) = 0 \quad (17)$$

After solving the hyperbolic step for the initial condition, the system advances one more time step by an ode solver. Then, for the next time step, the hyperbolic solver is used, and so on.

Instantaneous pressure-relaxation

Usually, values of the pressure-relaxation parameter r_P are unknown. Nevertheless, the presumption of the same pressure for two phases is widespread [27]. Such conditions can be reached by specifying a high value for r_P. But, instead of solving the system of ordinary differential eqs. (15)-(17), direct solving of the problem is numerically more efficient. Evje and Flatten [22] presented eq. (18) for instantaneous pressure relaxation:

$$\frac{R_g\rho_g}{\rho_{g(P)}}+\frac{R_l\rho_l}{\rho_{l(P)}}=1 \tag{18}$$

Instead of densities denominator, the quadratic equation for calculating the pressure term is obtained through substituted eq. (9):

$$\begin{aligned}&P^2+P[C_l^2(\rho_{0,l}-R_l\rho_l)+C_g^2(\rho_{0,g}-R_g\rho_g)-(P_{0,l}+P_{0,g})]-\\&-C_g^2C_l^2(R_g\rho_g\rho_{0,l}+R_l\rho_l\rho_{0,g}-\rho_{0,g}\rho_{0,l})-C_g^2P_{0,l}(\rho_{0,g}-R_g\rho_g)-\\&-C_l^2P_{0,g}(\rho_{0,l}-R_l\rho_l)+P_{0,g}P_{0,l}=0\end{aligned} \tag{19}$$

By solving the previous quadratic equation and selecting its positive root, the other variables such as ρ_g, ρ_l, R_g, R_l, u_g, and u_l can be calculated and can be used as the hyperbolic's initial values at the next time step. Note that $\rho_{k,0}$, $P_{k,0}$, and C_k are reference values for density, pressure, and sound speed in every phase, and the amount of these variables is equal to reference values presented in section *Single-pressure model* for the single-pressure model.

In the present study, the two-pressure model is presented as the two-pressure model 1 and the two-pressure model 2. In the two-pressure model 1, the finite pressure-relaxation procedure is used. Also, in the two-pressure model 2, instantaneous pressure relaxation is used.

Free pressure model

Most of the two-fluid models are characterized by the non-conservativeness of their governing equations. Therefore, these two-fluid models cannot be solved by conventional numerical techniques established for single-phase conservative systems. Therefore, new techniques are required for the numerical solution of these models.

To overcome this problem, Watson [4] presented a conservative form of the two-fluid model. The free pressure model consists of two differential equations: a total mass equation and a total momentum equation. In the presented free pressure model, the gas and liquid phases are assumed incompressible.

Total mass equation:

$$\frac{\partial}{\partial t}(\rho_lR_l+\rho_gR_g)+\frac{\partial}{\partial x}(\rho_lR_lu_l+\rho_gR_gu_g)=0 \tag{20}$$

Total momentum equation:

$$\frac{\partial}{\partial t}(\rho_l u_l + \rho_g u_g) + \frac{\partial}{\partial x}\left[\frac{1}{2}\rho_l u_l^2 - \frac{1}{2}\rho_g u_g^2 + (\rho_l - \rho_g)G\cos\beta h_l\right] = \\ = (\rho_l - \rho_g)G\sin\beta + \left(\frac{1}{R_l} + \frac{1}{R_g}\right)F_i + \frac{F_{gw}}{R_g} - \frac{F_{lw}}{R_l} \tag{21}$$

The unknowns in the free pressure equations system are R_g, R_l, u_g, and u_l. However, there are only two differential equations for this system. Hence, two additional algebraic equations are required. The first algebraic relation is a geometric constraint for two phases, and eq. (8) is used for them. In addition to the geometric constraint, another required:

$$\frac{\partial}{\partial x}(R_l u_l + R_g u_g) = 0 \tag{22}$$

According to eq. (22), one can conclude that this equation is only a function of time. This time function is represented by $C(t)$ and considered as a function of inlet flow parameters:

$$R_l u_l + R_g u_g = C(t) = (R_l u_l + R_g u_g)_{inlet} \tag{23}$$

where *inlet* is the inlet of the pipe.

Hyperbolic analysis of the two-fluid model

In the two-fluid model, the equations system can be mathematically classified *via* the characteristics analysis: that is, for the real characteristics, the equations are hyperbolic, and the system is well-posed. Conversely, the equations are elliptic for the complex characteristics, and the initial value problem is ill-posed.

In this section, the roots of the characteristic equation of the two-fluid model are presented. If this equation's roots are complex, then the initial value problem becomes ill-posed that is led to creating the unbounded instabilities, and as a result, the solution will not convergent. If the characteristic equation's roots are real, then the problem becomes well-posed and unbounded instabilities are eliminated [6].

Roots of the characteristic equation of the single-pressure model

Evje and Flatten [22] presented eq. (24) by using analysis of density perturbations for the eigenvalues in which eqs. (25)-(28) are governed [22].

$$\lambda_{(1,2)} = u_P \pm C_m, \quad \lambda_{(3,4)} = u_u \pm v \tag{24}$$

$$u_P = \frac{R_g\rho_l u_g + R_l\rho_g u_l}{R_g\rho_l + R_l\rho_g} \tag{25}$$

$$u_u = \frac{R_g\rho_l u_l + R_l\rho_g u_g}{R_g\rho_l + R_l\rho_g} \tag{26}$$

$$v = \sqrt{\frac{\Delta P\ (R_g\rho_l + R_l\rho_g) - R_g R_l \rho_l \rho_g (u_g - u_l)^2}{(R_g\rho_l + R_l\rho_g)^2}} \tag{27}$$

$$C_m = \sqrt{\frac{R_g\rho_l + R_l\rho_g}{\left(\frac{\partial\rho_g}{\partial P}\right)R_g\rho_l + \left(\frac{\partial\rho_l}{\partial P}\right)R_l\rho_g}} \tag{28}$$

Equation (27) shows that if ΔP is equal to zero, the eigenvalues are complex; thus, the system becomes ill-posed. Therefore, in eq. (7), we must have $\delta > 1$.

Roots of the characteristic equation of the two-pressure model

The eigenvalues are analytically obtained for the two-pressure model having five equations. These values are calculated by the following equation [27]:

$$\lambda = (u_i u_g - C_g u_g + C_g u_l - C_l u_l + C_l) \tag{29}$$

According to eq. (29), it is found that all eigenvalues are real, except in the situation that the two phase's speeds are equal. All eigenvalues are non-zero, and the system is strictly hyperbolic. A comprehensive discussion on eigenvalues of the five-equation model was presented in [27].

Roots of the characteristic equation of the free pressure model

The roots of the characteristic equation of the free pressure model are presented [1]:

$$\lambda_1 = \frac{(u_l + \chi u_g) - \sqrt{\Delta}}{1+\chi} \tag{30}$$

$$\lambda_2 = \frac{(u_l + \chi u_g) + \sqrt{\Delta}}{1+\chi} \tag{31}$$

In eqs. (30) and (31), Δ is presented:

$$\Delta = -\chi(u_g - u_l)^2 + (1+\chi)\frac{\Delta\rho\, G\cos\beta\, A_l}{\rho_l A_l^{'}} \geq 0 \tag{32}$$

Finally:

$$(u_g - u_l)^2 \leq \sqrt{\frac{\Delta\rho(\rho_l R_g + \rho_g R_l)}{\rho_g\rho_l} G\cos\beta\frac{A_l}{A_l^{'}}} \tag{33}$$

Roots of the presented characteristic equation are real, if $\Delta \geq 0$.

In fact, eq. (33) states Kelvin Helmholtz instability conditions. This equation shows that limit of stability in the free-pressure two-fluid models the same limit of Kelvin Helmholtz stability. The limit of well-posed of the single-pressure two-fluid model is similar to the limit

of the free pressure model [1]. In order to calculate the characteristic equation, the following equations are governed.

$$\Delta\rho = \rho_{\mathrm{l}} - \rho_{\mathrm{g}} \tag{34}$$

$$\chi = \frac{\rho_{\mathrm{g}} R_{\mathrm{l}}}{\rho_{\mathrm{l}} R_{\mathrm{g}}} \tag{35}$$

$$A_{\mathrm{l}}' = \frac{\mathrm{d}A_{\mathrm{l}}}{\mathrm{d}h_{\mathrm{l}}} \tag{36}$$

According to the characteristic equation's roots presented for the free pressure model and the single-pressure model, these models are in the situation that phase velocity difference does not exceed a specified limit. If the velocity difference of the two phases exceeds the allowed limit, the model becomes an ill-posed model, and a non-physical discontinuity is created in the solution field. This phenomenon is considered as the weakness of the two models. In the two-pressure model, the roots of the characteristic equation are real for all values. Therefore, the system has no hyperbolic condition.

Numerical method for solving governing equations

The governing equations of the three models discussed in section *Governing equations* can be categorized into two numerical formulations, and as a result, need different numerical methods. The free pressure model is known as conservative systems defined [33]:

$$\frac{\partial Q}{\partial t} + \frac{\partial F}{\partial x} = S \tag{37}$$

However, the single-pressure model and two-pressure model are non-conservative systems that can be expressed [33]:

$$\frac{\partial Q}{\partial t} + \frac{\partial F}{\partial x} = H\frac{\partial R_k}{\partial x} + S \tag{38}$$

where Q is a vector of conservative variables, F and S vectors represent the fluxes and source terms, respectively, and are algebraic functions of Q, and H is the interfacial pressure vector.

For the conservative system of eq. (37), the finite difference discretization results in the below expression:

$$Q_i^{n+1} = Q_i^n + \frac{\Delta t}{\Delta x}(F_{i-1/2}^{n\mathrm{Force}} - F_{i+1/2}^{n\mathrm{Force}}) + \Delta t\, S_i \tag{39}$$

For the non-conservative system of eq. (38), the finite difference discretization is:

$$Q_i^{n+1} = Q_i^n + \frac{\Delta t}{\Delta x}(F_{i-1/2}^{n\mathrm{Force}} - F_{i+1/2}^{n\mathrm{Force}}) + \Delta t\left(H\frac{\partial R_k}{\partial x}\right) + \Delta t\, S_i \tag{40}$$

In eqs. (39) and (40), n and $n+1$ show old and new time steps, respectively. Also, i is the cell. In order to calculate the numerical flux term $F_{i+1/2}^{n\mathrm{Force}}$, the force method is used.

Force numerical method

Toro [33] suggested a simple deterministic first-order centered method (force), in which the inter-cell flux is the average of the Richtmyer and the Lax-Friedrichs fluxes. Therefore, it is presented by:

$$F_{i+1/2}^{n\text{Force}} = \frac{1}{2}(F_{i+1/2}^{n\text{LF}} + F_{i+1/2}^{n\text{RI}}) \tag{41}$$

where $F_{i+1/2}^{n\text{LF}}$ is the Lax Friedrichs numerical flux and $F_{i+1/2}^{n\text{RI}}$ is the Ritchmyer numerical flux.

In the Lax Friedrichs method, the flux term is calculated [34]:

$$F_{i+1/2}^{n\text{LF}} = \frac{1}{2}(F_{i+1}^{n} + F_{i}^{n}) - \frac{\Delta x}{2\Delta t}(Q_{i+1}^{n} - Q_{i}^{n}) \tag{42}$$

In the Ritchmyer method, the flux term is calculated as following [34]:

$$F_{i+1/2}^{n\text{RI}} = F(Q_{i+1/2}^{n+1/2}) \tag{43}$$

$$Q_{i+1/2}^{n+1/2} = \frac{1}{2}(Q_{i}^{n} + Q_{i+1}^{n}) - \frac{\Delta t}{2\Delta x}(F_{i}^{n} - F_{i+1}^{n}) \tag{44}$$

Numerical flux in the i^{th} cell is expressed as $F_i^n = F(Q_i^n)$ and obtained based on the physical flux term.

The term $H\partial R_k/\partial x$ in single-pressure and the two-pressure equations is non-conservative and must be appropriately substituted. Improperly substituting this term causes instability in the solution [35]. For discretization of the non-conservative term $H\partial R_k/\partial x$, the following equations are presented [35]:

$$H\frac{\partial R_{\text{g}}}{\partial x} = HR_{\text{g}}R_{\text{l}}\frac{\partial BG}{\partial x} \tag{45a}$$

$$H\frac{\partial R_{\text{l}}}{\partial x} = HR_{\text{l}}R_{\text{g}}\frac{\partial BL}{\partial x} \tag{45b}$$

The derivative terms $\partial BG/\partial x$ and $\partial BL/\partial x$ are discretized by using a centered scheme.

$$HR_{\text{g}}R_{\text{l}}\frac{\partial BG}{\partial x} = HR_{\text{g}}R_{\text{l}}\frac{BG_{i+1} - BG_{i-1}}{2\Delta x} \tag{46a}$$

$$HR_{\text{l}}R_{\text{g}}\frac{\partial BL}{\partial x} = HR_{\text{g}}R_{\text{l}}\frac{BL_{i+1} - BL_{i-1}}{2\Delta x} \tag{46b}$$

Where

$$BG = \log\left(\frac{R_{\text{g}}}{R_{\text{l}}}\right) \tag{47a}$$

$$BL = \log\left(\frac{R_l}{R_g}\right) \tag{47b}$$

Calculation of time step

In order to calculate a time step, firstly, Δx is considered as mesh size using the following equation, then, Δt (*i.e.*, time step) is calculated [1]:

$$\Delta t = CFL\frac{\Delta x}{\lambda_{\max}^{n}} \tag{48}$$

In this work, the value of Courant Friedrichs Levy Number is assumed 0.4 to 0.5. The $\lambda_{\max}^{n}$ is the maximum value of the wave velocity in the solution field at the time *n*. Maximum wave velocity for the two-fluid model is equal to the maximum value of the characteristic equation of the governing equation in the solution field:

$$\lambda_{\max}^{n} = \max_{i}\left\{\max_{k}\left|\lambda_i^k\right|\right\} \quad for\ i = 1,\ldots, \quad M\ k = 1, Neq \tag{49}$$

where Neq is the number of system equations and λ_i^k is wave velocity in each computational mesh.

Numerical modeling

In this section, the water faucet case is used to compare the free-pressure two-fluid model, the single-pressure two-fluid model, and the two-pressure two-fluid model in which the pattern of annular two-phase flow is governed. This system includes a vertical pipe with a height of 12 m and a diameter of 1 m. Also, at the initial time, water velocity, air velocity, and volume fraction of water are 10, 0, and 0.8 m/s, respectively. The pressure at the pipe outlet is 100000 Pa. Inlet conditions are equivalent to the initial conditions. Furthermore, the fully developed boundary conditions are governed at the outlet of the pipe [36]. Figure 2 shows a schematic of the water faucet case.

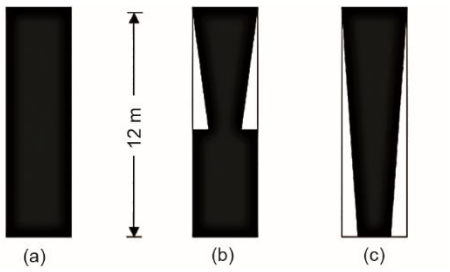

Figure 2. Schematic of water faucet case; (a) initial, (b) transient, and (c) steady-state

In this section, the transient analytical solution of the water faucet case is presented [1].

$$R_l(x,t) = \begin{cases} \dfrac{R_l^{\text{inlet}} u_l^{\text{inlet}}}{\sqrt{(u_l^{\text{inlet}})^2 + 2G(x - x^{\text{inlet}})}} & x \le x^{\text{inlet}} + u_l^{\text{inlet}} t + \dfrac{G}{2}t^2 \\ R_l^{\text{inlet}} \text{ otherwise} \end{cases} \tag{50}$$

$$u_l(x,t) = \begin{cases} \sqrt{(u_l^{\text{inlet}})^2 + 2G(x - x^{\text{inlet}})} & x \le x^{\text{inlet}} + u_l^{\text{inlet}} t + \dfrac{G}{2} \\ u_l^{\text{inlet}} + Gt \text{ otherwise} \end{cases} \tag{51}$$

where R_l^{inlet} is liquid phase volume fraction at the inlet of the pipe that is equal to 0.8. The term u_l^{inlet} is the liquid phase velocity at the inlet of the pipe that is equal to 10 m/s. Variable t is time, G – is the gravitational acceleration constant and x^{inlet} – the position at the inlet of the pipe, which is equal to zero. The reference solution was obtained from Evje and Flatten [24].

First, independent computing mesh solutions are presented for the gas phase volume fraction profile and liquid phase velocity profile for various two-fluid models. For all two-fluid models, computation time is 0.6 seconds, and the Courant Friedrichs Levy number is assumed to be 0.5.

Figures 3(a) and 3(b) show the gas volume fraction profile and the liquid velocity profile for the two-fluid free-pressure model, respectively.

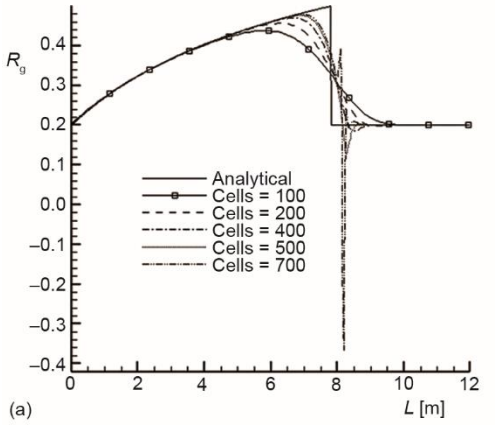

Figure 3(a). Independent solutions of computing mesh for gas-phase volume fraction profile, free pressure model

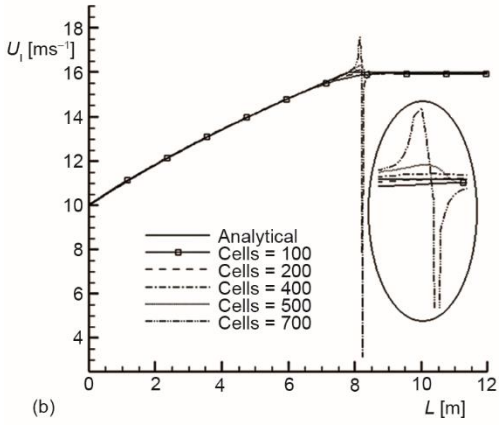

Figure 3(b). Independent solutions of computing mesh for liquid phase velocity profile, free pressure model

The results obtained from numerical modeling indicate non-physical instabilities. These instabilities will exponentially grow by increasing the number of meshes. These instabilities are due to the ill-posed of free pressure model in the given case. In this case, the pipe is vertical, therefore, cosβ in eq. (33) is zero.

According to eq. (33), when the two phases' velocities are equal, the free pressure model is well-posed. However, in the water faucet case, the velocities of the two phases are different. Thus, in the water faucet case, the mesh independent results cannot be obtained by using the free-pressure model.

Figures 4(a) and 4(b) show the gas phase volume fraction profile and the liquid phase velocity profile for the single-pressure two-fluid model, respectively. Figures 5(a) and 5(b) show the gas phase's volume fraction profile and the liquid phase's velocity profile for the two-pressure two-fluid model 2, respectively.

The free-pressure model is ill-posed in the desired physics. Therefore, the free-pressure model is neglected during the comparison process of the two-fluid model. The number of computational meshes is assumed to equal 5000. Although the criteria of well-posedness for the free pressure model are similar to that for the single-pressure model, unbounded instabilities have not been observed in the single-pressure model.

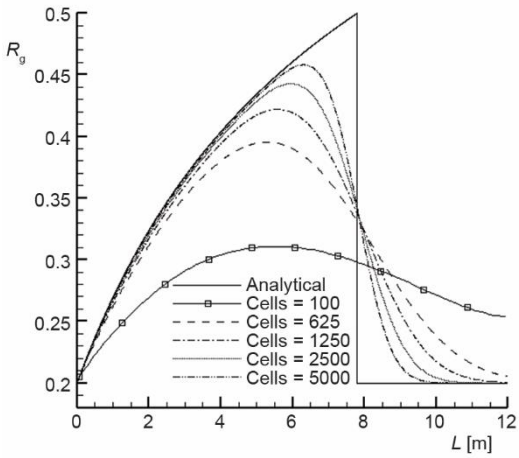

Figure 4(a). Independent solutions of computing mesh of the gas phase volume fraction profile, single-pressure model

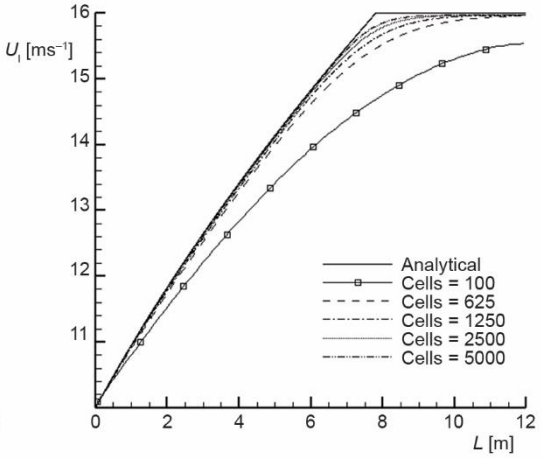

Figure 4(b). Independent solutions of computing mesh of the liquid phase velocity profile, single-pressure model

The single-pressure two-fluid model can properly predict the behavior of the two-phase flows that are weakly coupled together due to having two continuity equations and two momentum equations. Note that the wave propagation in each phase takes place at different velocities. This was illustrated correctly in the water faucet case, and no numerical jumps were observed.

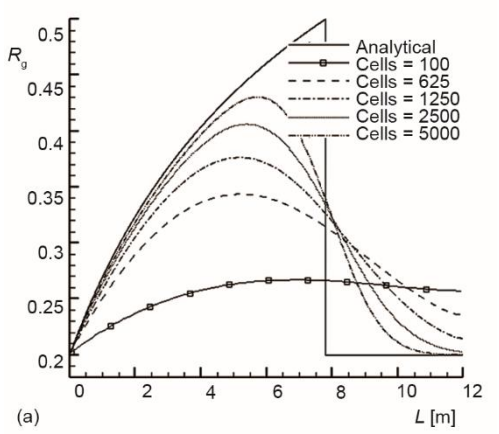

Figure 5(a). Independent solutions of computing mesh of the gas phase volume fraction profile, two-pressure model 2

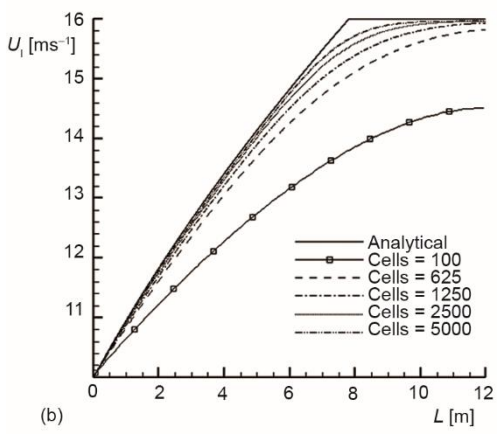

Figure 5(b). Independent solutions of computing mesh of the liquid phase velocity profile, two-pressure model 2

In the single-pressure model, if ΔP in eq. (27) is zero, then the roots of the characteristic equation (*i.e.* λ_3 and λ_4) are complex; as a result, the single-pressure model is ill-posed. In this situation, obtaining mesh independent results is impossible, and as the number of meshes increases, non-physical instabilities grow exponentially. In this condition, to deal with the single-pressure model's ill-posed problem, the two-pressure model 2 is proposed. According

to eq. (29), the two-pressure model 2 has the real and unconditional roots of the characteristic equation, and it is well-posed in all conditions.

In the free-pressure two-fluid model, the liquid and gas phases' densities are constant, but in the single-pressure two-fluid model, the liquid phase's density is constant. The density of the gas phase is variable. Since changes in the density of the gas phase are low, they can be neglected. Thus, the free-pressure model and the single-pressure model are physically in the same conditions, and the difference in the obtained results is due to the model's accuracy.

The free-pressure model in the water faucet case is ill-posed. Therefore, the free-pressure model is neglected for comparison of the two-fluid model.

The computational mesh number is assumed 5000 to compare the single-pressure, the two-pressure 1, and the two-pressure 2 of two-fluid models.

In this section, a comparison among the single-pressure model, the two-pressure model 1, and the two-pressure model 2 are presented. The results from the comparison of models are indicated in figs. 6-9 for the gas phase volume fraction profile, the liquid phase velocity profile, the gas phase velocity profile, and liquid phase volume fraction profile, respectively.

The number of the computational mesh is 5000. Also, computation time is 0.6 seconds, and the value of Courant Friedrichs Levy number is assumed 0.4.

In tab. 1, the values selected for the pressure-relaxation parameter in the two-fluid model 1 are presented.

Table 1. Values of pressure-relaxation parameter

Pressure-relaxation parameter	Value
r_{P1}	0.001
r_{P2}	0.0001
r_{P3}	0.00001
r_{P4}	0.000001
r_{P5}	0.0000001
r_{P6}	0

The results of the gas phase volume fraction profile, liquid phase velocity profile, gas-phase velocity profile, and liquid phase volume fraction profile are shown in figs. 6-9, respectively. As r_P increases, results for the two-pressure model 1 and the two-pressure model 2 are approached together, and transferring the two-pressure model 1 into the two-pressure model 2 has occurred uniformly.

Results of the two-pressure model 1 are highly dependent on r_P. The best choice, results for the two-pressure model 1 and the two-pressure model 2 are approached together. Selecting amount r_P is difficult because there are no criteria for selecting it.

The comparison of models are shown in figs. 6-9 for the gas phase volume fraction profile, liquid phase velocity profile, gas-phase velocity profile, and liquid phase volume fraction profile, respectively, it was found that the two-pressure 1 and the two-pressure 2 have the nature of numerical diffusion than the single-pressure model. This numerical diffusion was observed in the gas phase volume fraction profile, liquid phase velocity profile, gas-phase velocity profile, and liquid phase volume fraction profile.

In this section, the comparison between the single-pressure model and the two-pressure model is presented. In fig. 10, the comparison between two-pressure model 1 and two-pressure model 2 is performed. In fig. 11, the comparison between the single-pressure model and the two-pressure model 2 for pressure profile is performed.

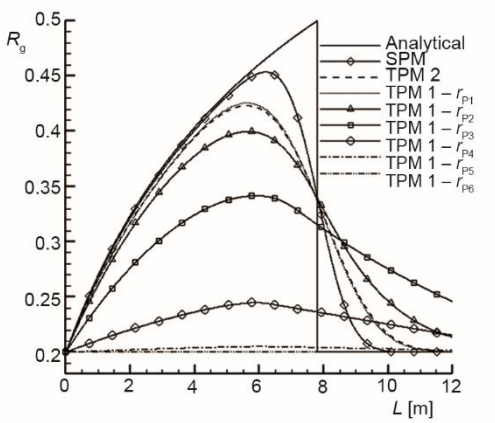

Figure 6. Comparison of various two-fluid models for the volume fraction profile of gas

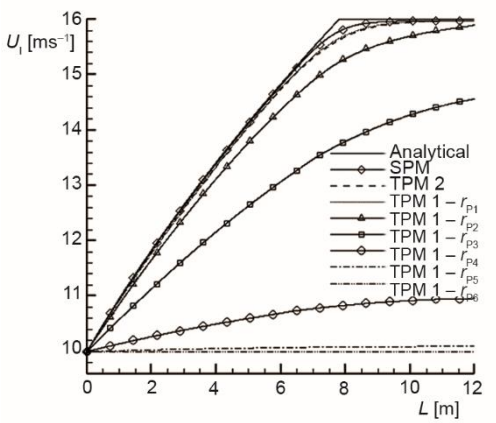

Figure 7. Comparison of various two-fluid models for the velocity profile of liquid phase

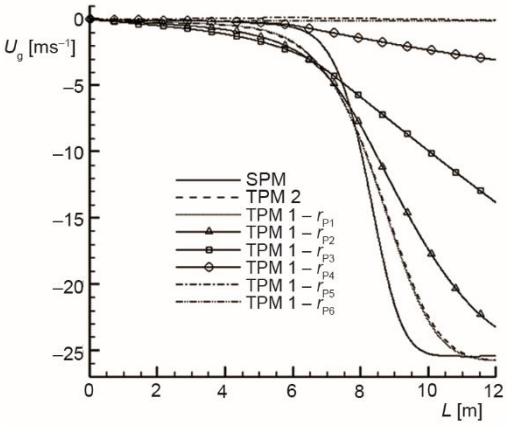

Figure 8. Comparison of various two-fluid models for velocity profile of gas phase

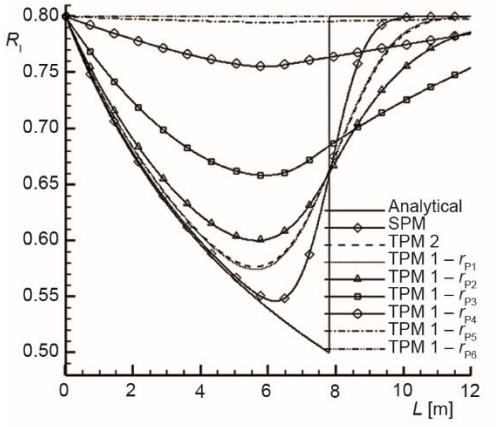

Figure 9. Comparison of various two-fluid models for the volume fraction profile of liquid-phase

The number of computation mesh is 5000. Also, computation time is 0.6 seconds, and the value of Courant Friedrichs Levy number is assumed 0.4.

Figure 11 indicates the comparison between the single-pressure model and the two-pressure model 2. Results show that similar to other flow variables (gas phase volume fraction and velocity profiles, liquid phase velocity, and volume fraction profile), the single-pressure model's pressure change profiles are predicted with higher accuracy than the two-pressure model 2.

The finite pressure relaxation method is used in two-pressure model 1, and gas and liquid phase pressures are not equal. Instantaneous pressure relaxation method is used in two-pressure model 2, and gas-phase pressure and liquid phase pressure are assumed the same.

Figure 10 shows that the pressure changes profile in the gas phase in the two-phase model 1 is predicted to be equal to that in the two-pressure model 2.

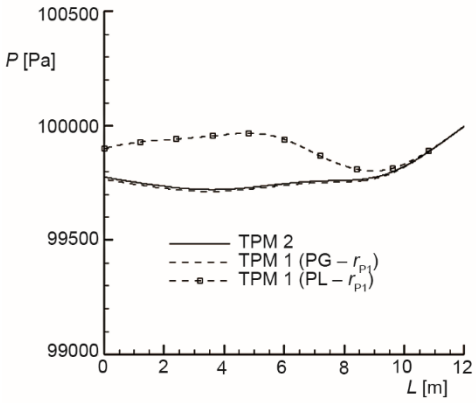

Figure 10. Comparison between the two-pressure model 1 and the two-pressure model 2 for pressure profile

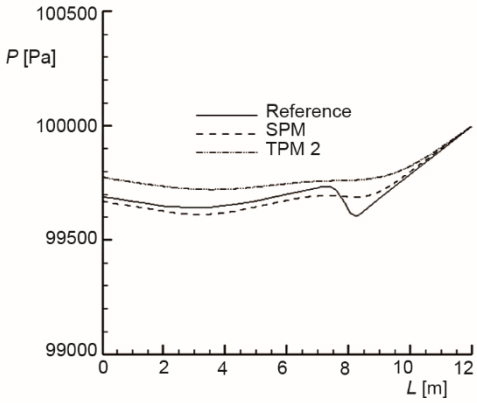

Figure 11. Comparison between the single-pressure model and the two-pressure model 2 for pressure profile

The volume fraction profile of gas and liquid phases is shown in figs. 6 and 9, respectively, as the volume fraction of gas increases, the volume fraction of liquid decreases. According to eq. (8), there is a direct relationship between the gas phase volume fraction and the liquid phase volume fraction. Thus, based on Bernoulli's equation, as the volume fraction of the gas-phase increases, the liquid phase pressure loss occurs, and the volume fraction of the gas phase decreases. The liquid phase pressure increases.

Therefore, according to the presented results of the volume fraction profiles of gas and liquid phases in figs. 6 and 9, respectively, in the inlet of pipe, the liquid phase's cross-section is larger than the gas phase's cross-section. Therefore, according to Bernoulli's equations, the liquid phase pressure must be higher than the gas phase pressure. It is shown in fig. 10. The liquid phase pressure decreases as the liquid phase volume fraction decreases due to Bernoulli's equations.

In the two-pressure model 1, the gas and liquid phases' pressure is not assumed the same. The assumption of inequality of phase's pressure is exact, and it corresponds to the flow's actual physics.

Flow evolution

The computations were performed for multiple time-step sizes to show the convergence of various two-fluid models in the time domain. For particular boundary and initial conditions of the simulation case, after 0.85 seconds solution reached a theoretical steady state. Then, the computations were performed for more than 1.0 seconds afterward to check the steady state convergence [1].

For comparison of the presented two-fluid models, the gas volume fraction profile and the liquid phase's velocity profile are presented in figs. 12 and 13, respectively. Various two-fluid models are compared in computational times 0.25, 0.75, and 1.0 seconds.

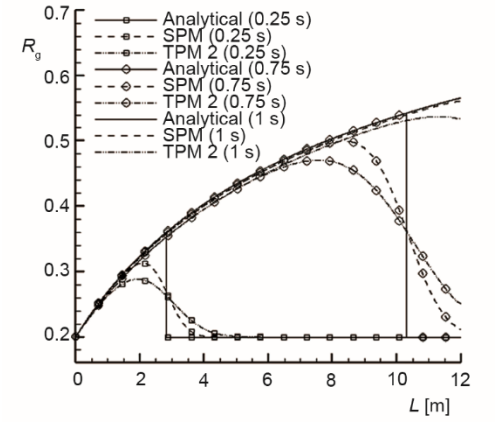

Figure 12. Time evolution of the volume fraction profile of gas-phase

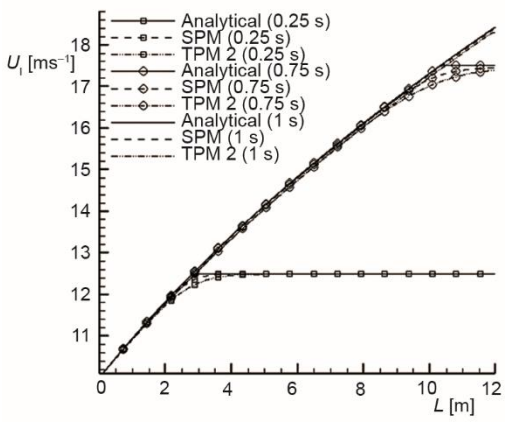

Figure 13. Time evolution of the velocity profile of liquid phase

Numerical results are presented for the gas phase's volume fraction profile, and the liquid velocity phase profile is presented in figs. 12 and 13, respectively. It can be seen that, at different computational times, the single-pressure model predicts more accurately the gas phase volume fraction and velocity profile of the liquid phase than the exact solution.

In the steady-state, the two-pressure model produces numerical diffusion in the solution field, leading to less precision of two-phase variables than single-pressure in numerical modeling.

Conclusions

The free-pressure two-fluid model is a conservative medal. It has no complexity related to the discretization of the non-conservative term existence in the single-pressure and the two-pressure model. A free-pressure model can exactly predict discontinuities in the solution field when the initial conditions satisfy the Kelvin Helmholtz instability condition. The free-pressure model has two crucial weaknesses: neglecting the compressibility of the gas phase and lack of predicting the phase's pressure profile changes in the output of the model.

A single-pressure two-fluid model, due to having two continuity equations and two equations of momentum, can properly predict the behavior of flows that are weakly coupled together in two phases so that propagation wave is performed in each phase at different velocities. It was demonstrated in the water faucet case, and no other jump in the flow variables was observed.

The two-pressure two-fluid model is well-posed unconditionally. The two-pressure models have more numerical diffusion than the single-pressure models. Also, high numerical diffusion was led to better mismatches of the solutions by analyzing the problem.

The two-pressure model 1 is strongly dependent on the value of r_P and in the best choice of r_P, the two-phase model 1. The solutions for predicting the flow variables (gas and liquid phases volume fraction profile, gas and liquid phases velocity profile) are approximately equal to the two-pressure model 2.

One of the difficulties with the two-factor model 1 is the selection of the value of r_P because there is no specific criterion for selecting it. The assumption of the inequality of pressure of the phases is exact, and it is following the actual physics of the flow. Therefore, the

predicted pressure changes profile in the two-pressure model 1 is more consistent with actual physics.

References

[1] Omgba-Essama, C., Numerical Modeling of Transient Gas-Liquid Flows (Application to Stratified & Slug Flow Regimes), Ph. D. thesis, Cranfield University, Cranfield, IK, 2004
[2] Ishii, M., Mishima, K., Two-Fluid Model and Hydrodynamic Constitutive Relations, *Nuclear Engineering and Design, 82* (1984), 2, pp. 107-126
[3] Liao, J., *et al.*, A Study on the Numerical Stability of the Two-Fluid Model Near Ill-Posedness, *International Journal of Multiphase Flow, 34* (2008), 11, pp. 1067-1087
[4] Watson, M., Non-Linear Waves in Pipeline Two-Phase Flows, *Processing*, 3rd International Conference on Hyperbolic Problems, Uppsala, Sweden, 1990
[5] Stuhmiller, J., The Influence of Interfacial Pressure Forces on the Character of Two-Phase Flow Model Equations, *International Journal of Multiphase Flow, 3* (1977), 6, pp. 551-560
[6] Ransom, V. H., Hicks, D. L., Hyperbolic Two-Pressure Models for Two-Phase Flow, *Journal of Computational Physics, 53* (1984), 1, pp. 124-151
[7] Ansari, M., Shokri, V., Numerical Modeling of Slug Flow Initiation in a Horizontal Channels Using a Two-Fluid Model, *International Journal of Heat and Fluid Flow, 32* (2011), 1, pp. 145-155
[8] Bonzanini, A., D. *et al.*, Simplified 1D Incompressible Two-Fluid Model with Artificial Diffusion for Slug Flow Capturing in Horizontal and Nearly Horizontal Pipes, *Energies, 10* (2017), 9, 1372
[9] Holmas, H., Numerical Simulation of Transient Roll-Waves in Two-Phase Pipe Flow, *Chemical Engineering Science, 65* (2010), 5, pp. 1811-1825
[10] Holmas, H., *et al.*, Analysis of a 1D Incompressible Two-Fluid Model Including Artificial Diffusion, *IMA Journal of Applied Mathematics, 73* (2008), 4, pp. 651-667
[11] Louaked, M., *et al.*, Well-Posedness of Incompressible Models of Two-And Three-Phase Flow, *IMA Journal of Applied Mathematics, 68* (2003), 6, pp. 595-620
[12] Woodburn, P., Issa. R., Well-Posedness of One-Dimensional Transient, Two-Fluid Models of Two-Phase Flows, *Proceedings*, 3rd International Symposium on Mulitphase Flow, ASME Fluids Engineering Division Summer Meeting, Washington, D. C., USA, 1998
[13] Issa, R., Kempf, M., Simulation of Slug Flow in Horizontal and Nearly Horizontal Pipes with the Two-Fluid Model, *International Journal of Multiphase Flow, 39* (2003), 1, pp. 69-95
[14] Ansari, M., Shokri, V., New Algorithm for the Numerical Simulation of Two-Phase Stratified Gas-Liquid Flow and Its Application for Analyzing the Kelvin-Helmholtz Instability Criterion with Respect to Wavelength Effect, *Nuclear Engineering and Design, 237* (2007), 24, pp. 2302-2310
[15] Bonizzi, M., Issa, R., A Model for Simulating Gas Bubble Entrainment in Two-Phase Horizontal Slug Flow, *International Journal of Multiphase Flow, 29* (2003), 11, pp. 1685-1717
[16] Bonizzi, M., Issa, R., On the Simulation of Three-Phase Slug Flow in Nearly Horizontal Pipes Using the Multi-Fluid Model, *International Journal of Multiphase Flow, 29* (2003), 11, pp. 1719-1747
[17] Carneiro, J., Nieckele, A., Investigation of Slug Flow Characteristics in Inclined Pipelines, *Computational Methods in Multiphase Flow IV, 56* (2007), 4, pp. 185-194
[18] Emamzadeh, M., Issa, R. I., One-Dimensional Model for Numerical Simulation of Annular Flow in Horizontal and Vertical Pipes, *Multiphase Science and Technology, 25* (2013), 1, pp. 25-56
[19] Emamzadeh, M., Issa, R. I., A Model for Predicting the Transition Between Stratified and Annular Flow in Horizontal Pipes, *Multiphase Science and Technology, 25* (2013), 1, pp. 70-100
[20] Han, P., Guo, L., Numerical Simulation of Terrain-Induced Severe Slugging Coupled by Hydrodynamic Slugs in a Pipeline-Riser System, *International Journal of Heat and Fluid Flow, 56* (2015), Dec., pp. 355-366
[21] Shokri, V., Esmaeili, K., Comparison of the Effect of Hydrodynamic and Hydrostatic Models for Pressure Correction Term in Two-Fluid Model in Gas-Liquid Two-Phase Flow Modeling, *Journal of Molecular Liquids, 237* (2017), July, pp. 334-346
[22] Evje, S., Flatten, T., Hybrid Flux-Splitting Schemes for a Common Two-Fluid Model, *Journal of Computational Physics, 192* (2003), 1, pp. 175-210
[23] Paillere, H., *et al.*, On the Extension of the AUSM+ Scheme to Compressible Two-Fluid Models, *Computers & Fluids, 32* (2003), 6, pp. 891-916

[24] Evje, S., Flatten, T., Hybrid Central-Upwind Schemes for Numerical Resolution of Two-Phase Flows, *ESAIM: Mathematical Modelling and Numerical Analysis, 39* (2005), 2, pp. 253-273
[25] Munkejord, S. T., Comparison of Roe-Type Methods for Solving the Two-Fluid Model with and Without Pressure Relaxation, *Computers & fluids, 36* (2007), 6, pp. 1061-1080
[26] Zeng, Q., *et al.*, Comparison of Implicit and Explicit AUSM-Family Schemes for Compressible Multiphase Flows, *International Journal for Numerical Methods in Fluids, 77* (2015), 1, pp. 43-61
[27] Munkejord, S. T., Analysis of the Two-Fluid Model and the Drift-Flux Model for Numerical Calculation of Two-Phase Flow, Ph. D. thesis, NTNU, Trondheim, Norway, 2006
[28] Saurel, R., Abgrall, R., A Multiphase Godunov Method for Compressible Multifluid and Multiphase Flows, *Journal of Computational Physics, 150* (1999), 2, pp. 425-467
[29] Baer, M., Nunziato, J., A Two-Phase Mixture Theory for the Deflagration-to-Detonation Transition (DDT) in Reactive Granular Materials, *International Journal of Multiphase Flow, 12* (1986), 6, pp. 861-889
[30] Fontalvo, E. M., *et al.*, Assessment of Closure Relations on the Numerical Predictions of Vertical Annular Flows with the Two-Fluid Model, *International Journal of Multiphase Flow, 126* (2020), May, 103243
[31] Saraswat, S., *et al.*, Linear Stability Analysis of RELAP5 Two-Fluid Model in Nuclear Reactor Safety Results, *Annals of Nuclear Energy, 149* (2020), Dec., 107720
[32] Cortes, J., *et al.*, A Density Perturbation Method to Study the Eigenstructure of Two-Phase Flow Equation Systems, *Journal of Computational Physics, 147* (1998), 2, pp. 463-484
[33] Toro, E. F., *Riemann Solvers and Numerical Methods for Fluid Dynamics: A Practical Introduction*, Springer Science & Business Media, New York, USA, 2013
[34] Hirsch, H., Numerical Computation of Internal and External Flows, in: *Computational Methods for Inviscid and Viscous Flows*, Willy, New York, USA, 1990, Vol. 2, pp. 536-556
[35] Coquel, F., *et al.*, A Numerical Method Using Upwind Schemes for the Resolution of Two-Phase Flows, *Journal of Computational Physics, 136* (1997), 2, pp. 272-288
[36] Ransom, V., Numerical Benchmark Test no. 2.3: Expulsion of Steam by Sub-Cooled Water, Multiphase *Science and Technology, 3* (1987), 1-4, pp. 471-473

Paper submitted: April 20, 2020
Paper revised: March 12, 2021
Paper accepted: March 28, 2021